Limited Proteolysis of *Salmonella typhimurium* Nicotinic Acid Phosphoribosyltransferase Reveals ATP-Linked Conformational Change†

Mathumathi Rajavel,‡ Jeffrey Gross,‡ Edy Segura,‡ William T. Moore,§ and Charles Grubmeyer*,‡

Department of Biochemistry and Fels Research Institute, Temple University School of Medicine, 3420 North Broad Street, Philadelphia, Pennsylvania 19140, and Department of Pathology and Laboratory Medicine, Protein Chemistry Laboratory, The School of Medicine, University of Pennsylvania, Philadelphia, Pennsylvania 19104

Received August 1, 1995; Revised Manuscript Received November 16, 1995⊗

ABSTRACT: Nicotinic acid phosphoribosyltransferase (NAPRTase; EC 2.4.2.11) couples stoichiometric ATP hydrolysis with formation of nicotinate mononucleotide (NAMN) from nicotinic acid and α-D-5-phosphoribosyl 1-pyrophosphate (PRPP). Trypsin rapidly inactivated the ATPase and NAMN synthesis activities of NAPRTase in parallel, with cleavages at Arg-384 and Lys-374 of the 399-residue protein. ATP and PRPP each provided protection against tryptic cleavage. Limited chymotryptic proteolysis of NAPRTase exhibited very similar behavior, with specific cleavage at Phe-382 and protection by substrates. Results suggest that a solvent-exposed loop encompassing Lys-374, Phe-382, and Arg-384 is protected by ATP- or PRPP-induced conformational changes. The ability of ATP to protect even under conditions in which enzyme phosphorylation was prevented by EDTA provides evidence for a distinct ATP-induced protein conformation that acts as an intermediate in energy coupling.

The use of ATP hydrolysis to drive enzymatic reactions requires a mechanism to couple hydrolytic bond energy to the linked process. The mechanism of energy coupling divides ATPases into two groups (Tanford, 1983): those enzymes which chemically couple ATP hydrolysis by phosphorylation of a substrate-derived enzymic intermediate and those in which the coupling does not involve substrate phosphorylation and is apparently conformational. The former group is relatively easy to understand once the chemical intermediates are identified. For example, glutamine synthetase uses ATP to phosphorylate glutamate, rendering it susceptible to nucleophilic attack by ammonia (Meek & Villafranca, 1982). In the second group, which includes ion-pumping ATPases and a variety of other enzymes, it is less clear how energy coupling occurs. Previous studies of conformational coupling have focused mainly on the ion-pumping ATPases (Jencks, 1980; 1989; Tanford, 1983). Jencks (1980) has proposed that coupling requires only a compulsory intertwining of two processes, with "rules" preventing uncoupled events. In this context, if a distinct conformational state is required for a step in one of the two reactions and that state is only generated by a step in the other reaction, then energetic coupling between the two reactions will result.

It has become clear that conformational coupling is not limited to ion transporters and molecular motors and is much more ubiquitous than previously realized. In recent years a variety of enzymes (Table 1) have been identified that fall into this class; most utilize ATP hydrolysis to carry out a recognition process. Examples include ATP-dependent proteases (Armon et al., 1990), the chaperonins GroEL (Martin et al., 1991) and DnaK (Szabo et al., 1994), RecA (West, 1992; Nguyen et al., 1993), periplasmic bacterial transport systems (Ames, 1990), and DNA gyrases (Cullis et al., 1992; Yodh & Bryant, 1993). In all cases ATP hydrolysis is proposed to drive a cycle of affinity changes that allows binding and release of secondary ligands.

Salmonella typhimurium nicotinate phosphoribosyltransferase (NAPRTase; EC 2.4.2.11)[1] is a metabolic enzyme that couples ATP hydrolytic energy to synthesis of nicotinate mononucleotide (NAMN) using a similar cycle of affinity changes (Vinitsky & Grubmeyer, 1993). NAPRTase carries out formation of the NAD precursor NAMN and PP_i from 5-phosphoribosyl 1-pyrophosphate (PRPP) and nicotinic acid (NA). Native NAPRTase has very low affinity for PRPP and NA substrates and a low k_{cat}. However in the presence of ATP, a phosphoenzyme is formed and NAPRTase acquires high affinity for substrates PRPP and NA. Rapid catalysis to form NAMN and PP_i occurs, and the nascent PP_i triggers hydrolytic cleavage of E-P to produce a loosely associated products complex which then dissociates. The presence of ATP causes 2000-fold increases in k_{cat}/K_M for each substrate, and also supports a 1640-fold increase in the steady-state ratio of [NAMN][PP_i]/[PRPP][NA]. It has not yet been determined whether the effects of ATP are associated with protein conformational changes. It is also not clear whether it is E-P formation, or ATP binding alone, that is required to trigger the affinity changes associated with substrate binding. The ATPase and NAMN synthesis

† This research was supported by a grant from the National Science Foundation (DMB-9103029). Facilities in the Fels Institute for Cancer Research and Molecular Biology are supported by NIH5-P30-CA12227. Mass spectrometry was provided by the Protein Chemistry Laboratory of the Medical School of the University of Pennsylvania supported by core grants of the Diabetes and Cancer Centers (DK-19525 and CA-16520). J.G. is the recipient of a Temple University Fellowship.

* To whom correspondence should be addressed. Tel: (215) 707-4495. FAX: (215) 707-7536. E-mail: ctg@ariel.fels.temple.edu.

‡ Temple University.

§ University of Pennsylvania.

⊗ Abstract published in *Advance ACS Abstracts,* March 1, 1996.

[1] Abbreviations: DTT, dithiothreitol; NA, nicotinic acid; NAMN, nicotinic acid mononucleotide; NAPRTase, nicotinic acid phosphoribosyltransferase; PMSF, phenylmethylsulfonyl fluoride; PRPP, α-D-5-phosphoribosyl 1-pyrophosphate; PRTase, phosphoribosyltransferase.

0006-2960/96/0435-3909$12.00/0

Table 1: ATP Hydrolysis Coupled to Affinity Changes

protein	function	transduction	reference
Rho	transcription termination	ATP hydrolysis causes cycle of RNA affinity changes	Stitt (1988)
Lon	specific proteolysis	ATP hydrolysis coupled to binding and release of target protein	Armon et al. (1990)
RecA	strand exchange in recombination	ATP hydrolysis coupled to DNA strand exchange	Nguyen et al. (1993); West (1992)
GroEL	prevents protein aggregation	ATP hydrolysis coupled to protein binding and release	Martin et al. (1991)
DNA helicase II	unwinding DNA	helicase II-promoted DNA unwinding reaction dependent on ATP hydrolysis	Yodh and Bryant (1993); Cullis et al. (1992)
DnaK	protein folding	binding and release of target protein coupled to ATP hydrolysis	Szabo et al. (1994)

functions of NAPRTase may not be intimately related: although in the yeast enzyme NAMN synthesis does not proceed without ATP hydrolysis (Hanna et al., 1983; Kosaka et al., 1971, 1977), in the human (Niedel & Dietrich, 1973; Smith & Gholson, 1969) and *S. typhimurium* (Vinitsky & Grubmeyer, 1993) enzymes uncoupled NAMN synthesis can be readily detected. In a protozoal NAPRTase, no effect of ATP is noted (Khan et al., 1967).

In the last year high-resolution crystal structures of several PRTases have become available. *S. typhimurium* orotate PRTase (Scapin et al., 1994) and human hypoxanthine-guanine HGPRTase (Eads et al., 1994) were solved by our collaborators, and glutamine amido PRTase was solved by Smith et al., (1994). The former two are relatively small enzymes (213 and 216 amino acids, respectively) with simple structures in which a modified nucleotide binding fold is fused to an amino or carboxy subdomain that functions in base recognition. In the case of glutamine amido PRTase, the PRTase domain is fused to a structurally distinct amino-terminal glutaminase domain (Smith et al., 1994). The 399-residue NAPRTase (whose structure has not yet been detemined) might thus have a domain architecture with separate structures for ATPase and PRTase substrate binding or might consist of a single domain with subsites for the ligands.

Here, we have examined the effects of partial proteolysis on both ATP hydrolysis and NAMN synthesis activities. We show that NAPRTase is extremely sensitive to trypsin and chymotrypsin, with both ATPase and NAMN synthesis activities inactivated by the removal of a carboxy-terminal 25 or 17 amino acids. Protection by ATP provides evidence for a conformational change associated with ATP binding.

EXPERIMENTAL PROCEDURES

Materials. Bacterial growth media were from Difco. Restriction enzymes and T4 DNA ligase were obtained from New England Biolabs. Taq DNA polymerase and dNTPs were purchased from Perkin Elmer. Lactate dehydrogenase and pyruvate kinase were from Boehringer-Mannheim. TPCK-treated trypsin was from Worthington. Chymotrypsin, other biochemicals, and [^{14}C]nicotinic acid were obtained from Sigma. Inorganic chemicals and chromatography solvents were purchased from Fisher. Customized primers were synthesized at the DNA synthesis facility of Temple University School of Medicine. T7 primers used for *pncB* sequencing were obtained from Novagen.

Bacterial Strains, Plasmids, and Culture Conditions. S. typhimurium RM926 (*hsdLT(r$^-$m$^+$), hsdSA(r$^-$m$^+$), metE551, trpD2, leu, val, rpsL120, galE*) was donated by Russell Maurer. Plasmid pRSET C was from Invitrogen, and plasmid pGP1-2 (Tabor & Richardson, 1985) was a gift from Stanley Tabor. Plasmid pC18 was as desribed by Vinitsky et al. (1991). RM926/pGP1-2 and RMS01 (described below) were grown at 30 °C.

Conventional recombinant DNA techniques were performed as described in Sambrook et al. (1989). DNA purification was carried out with a Qiagen plasmid purification kit. Dideoxy DNA sequencing was carried out with Sequenase (USB) as described by the manufacturer. PCR reactions were carried out as described by the manufacturer (Perkin Elmer) in a Coy thermal cycler.

Construction of pncB Overexpression Plasmid pRM17.1. The overexpression plasmid pRM17.1 was constructed as follows: the *pncB* coding sequence was PCR amplified from pC18 (Vinitsky et al., 1991) using DNA oligomers (clockwise primer 5′-CAACAGCGCA*CATATG*ACACAATTC-3′ and counterclockwise primer 5′-CACAGG*CCATGG*TTAACT-TGC-3′). These primers contain restriction sites (italicized) for *Nde*I at the 5′ end and *Nco*I at the 3′ end of the amplified fragment. The amplified fragment was restriction digested with these enzymes and ligated to similarly digested T7 expression vector pRSET C. *S. typhimurium* strain RM926 was transformed with the ligated mixture, and ampicillin-resistant transformants were screened for recombinants containing the insert by plasmid extractions and restriction digestion. After identifying the correct clone (pRM17) carrying *pncB*, the 852 bp *Nru*I−*Kpn*I fragment (nt161−1013) was replaced from pC18. The resultant construct, designated pRM17.1, contained only the coding sequence of *pncB* and was sequenced using T7 promoter and T7 terminator primers across the *Nru*I and *Kpn*I sites. The replacement cloning minimized the region of *pncB* to be sequenced in order to ensure that no undesired mutations had occurred during PCR amplification. Plasmid pGP1-2, containing the T7 RNA polymerase gene under the control of the λ P_L promoter regulated by a temperature sensitive cI857 repressor, was used for the overexpression of the protein. RM926 containing pGP1-2 was transformed with pRM17.1 and the resultant kanamycin- and ampicillin-resistant transformant, designated RMS01, gave a high level expression of *pncB.*

Purification of NAPRTase. The purification of NAPRTase was as described earlier (Vinitsky & Grubmeyer, 1993) with slight modifications. *S. typhimurium* strain RMS01 was grown overnight in 12 L of tryptone broth (Davis et al., 1980) containing 100 μg of ampicillin/mL and 75 μg of kanamycin/mL at 30 °C. Cells (21 g) were harvested by centrifugation and resuspended in 42 mL of 200 mM sodium phosphate (NaP_i), pH 8.0, containing 1 mM PMSF and 1 mM DTT. In an ice bath, cells were disrupted by three 2-min pulses with a Heat Systems-Ultrasonics W185 sonicator at full power. Debris was removed by centrifugation at 27 000*g* for 20 min. The supernatant was treated as described earlier (Vinitsky & Grubmeyer, 1993) until the first chromatographic step.

For chromatography, the 60% saturation ammonium sulfate pellet was dissolved in buffer A (10 mM NaP_i, 10 mM Tris-HCl, pH 8.0, 0.1 mM DTT, 10% glycerol). Coupled spectrophotometric ATPase assays (Vinitsky & Grubmeyer, 1993) at this point showed a high basal level of ATPase activity in the absence of NA and additional NA-dependent activity. The protein sample was desalted by overnight dialysis against four changes (4 L) of buffer A. The desalted protein was applied onto a Q-Sepharose column (Pharmacia; 2.6 × 10 cm) and eluted with a 280 mL linear gradient of 0%−100% buffer B (buffer A containing 1 M NaCl). NAPRTase eluted at approximately 0.3 M NaCl.

The active fractions from the Q-Sepharose column were pooled and brought to 70% saturation with ammonium sulfate. After centrifugation the pellet was resuspended with buffer containing 100 mM NaP_i, pH 8.0, 10% glycerol, 1 mM DTT and 30% saturated ammonium sulfate. Sufficient volume of 100 mM NaP_i pH 8.0, 10% glycerol, and 1 mM DTT was added to solubilize the pellet. The protein was then loaded onto a phenyl Sepharose column (Pharmacia; 1.6 × 10 cm) pre-equilibrated with buffer containing 100 mM NaP_i, 1 mM DTT, 10% glycerol, and 30% saturated ammonium sulfate. The protein was eluted with a 150 mL linear gradient of 30%−0% saturated ammonium sulfate in the same buffer. NAPRTase began to elute at 100% B. To elute the remaining protein, a buffer containing 50 mM NaP_i, 10% glycerol, and 0.5 mM DTT was employed. The active fractions showed negligible basal ATPase activity. The purified enzyme was stored at 4 °C as a 70% saturated ammonium sulfate suspension in 200 mM NaP_i buffer, pH 8.0, containing 10% glycerol and 5 mM DTT.

Assay of Enzymatic Activity. Coupled spectrophotometric ATPase assays were performed as described by Vinitsky and Grubmeyer (1993). The [^{14}C]NA label transfer procedure of Preiss and Handler (1958) was performed in a 0.1 mL total volume at 30 °C as described earlier (Vinitsky & Grubmeyer, 1993). A 2 μg amount of native enzyme and 10 μg of the cleaved enzyme were employed in the coupled (ATP present) and uncoupled (ATP absent) reactions, respectively. Aliquots (10 μL) of the reactions at various time intervals were spotted on the Whatman No. 3MM paper, which was prespotted with 2 μL of 30% perchloric acid, and the samples were resolved with 1 M ammonium acetate, pH 5.0:100% ethanol (3:7). The chromatogram was developed in a Fuji Bioimage Analyzer BAS 2000. Rates of NAMN synthesis were calculated from the percentage conversion of the substrate obtained from the digitized photostimulated luminescence measurements and were expressed in units per mg of protein. A unit of activity is defined as that amount of enzyme catalyzing the conversion of 1 μmol of NA per min under the conditions given. ATP/ADP exchange reactions were carried out as described (Vinitsky & Grubmeyer, 1993) but with [^{14}C]ADP. The assay of PP_i-stimulated ATPase was conducted as for coupled ATPase, except PRPP was omitted and PP_i was added to 1 mM. Protein measurements were done spectrophotometrically using $E^{0.1\%}_{280nm} = 1.27$ (Vinitsky & Grubmeyer, 1993).

Enzyme Phosphorylation. Native, trypsin-treated, and chymotrypsin-treated NAPRTase were assayed for phosphorylation with [γ-^{32}P]ATP as described in the accompanying paper (Gross et al., 1996).

Proteolytic Digestion of NAPRTase. The purified protein was desalted on 1 mL centrifuge columns (Penefsky, 1977) in buffer containing 200 mM K-glutamate, 20 mM Tris-HCl, 5 mM DTT, pH 8.3. After a 5 min pre-incubation of the samples in a 30 °C water bath, either trypsin or chymotrypsin (protease to protein ratio of 1:200, w/w) was added from a 10 mg/mL stock in 1 mM HCl, and incubations were continued. In experiments with chymotrypsin, 5 mM $CaCl_2$ was also present in the reaction buffer. Aliquots were removed at various time intervals, and proteolysis was stopped by adding PMSF to 0.1 mM from a 2.5 mM stock in 2-propanol.

N-Terminal Sequencing. The native and the cleaved proteins were purified on a C4 reverse phase column (Vydac 214TP54), driven by a Waters 600E controller and pump system with detection at 215 and 280 nm by a Waters 490 detector. Solvent A was 0.1% trifluoroacetic acid in water and solvent B was 0.1% trifluoroacetic acid in acetonitrile. Elution at a flow rate of 1.0 mL/min was performed using a 60 min linear gradient from 0% to 100% solvent B. The acquired data were stored and analyzed by the Waters Maxima 820 software package. The collected peaks were dried under vacuum and reconstituted with 50 μL of 60% ACN. A portion (10 μL) of the purified peptide was applied to a 2090E Porton microsequencer interfaced with a Hewlett-Packard 1090 HPLC for PTH−amino acid identification and quantification.

Mass Spectrometry. Samples of the N-terminal fragments for mass analysis were prepared by proteolytic digestion and HPLC exactly as for N-terminal sequencing. When the C-terminal fragments were to be analyzed, the digestion mixture was applied directly to the mass spectrometer.

Electrospray ionization mass spectrometry (ESI-MS) was performed on a Fisons Instruments (Beverly, MA) VG Quattro triple-quadrupole mass spectrometer outfitted with the manufacturer's electrospray source. For the larger molecular weight intact proteins and fragments mass analysis were made using only Q1. The coaxial nebulizer gas flow was 10 L/h, the drying gas flow was set at 300 L/h, and the source temperature was maintained at 80 °C. Samples were diluted 1/10 to 1/50 in 50% acetonitrile and 1% formic acid in water, and each was injected as a 10 μL bolus into a stream of matrix consisting of 50% acetonitrile and 1 mM triethylamine to permit a family of lower charge state distributions. Matrix flow was established at 12 μL/min by a Harvard Apparatus (South Natick, MA) model 55−3206 microliter syringe pump. In most cases 10 scans were acquired per sample and averaged over the mass (m/z) range 800−2000 using a scan rate of 4.91 s/scan. Analyses were performed in the positive ion mode with typical operating voltages set at 3.74 kV on the capillary and 0.49 kV on the high-voltage lens in the electrospray source. The first quadrupole was calibrated using equine myoglobin and data were processed using Fisons Instruments MassLynx software.

Matrix-assisted laser desorption ionization mass spectrometry (MALDI-MS) was performed on a Fisons Instruments VG TofSpec time-of-flight mass spectrometer outfitted with an N2 (337 nm) laser. Samples were analyzed using a matrix of α-cyano-4-hydroxycinnamic acid. Ions were accelerated with a potential of 20 kV. Mass calibrations were established using synthetic peptides covering the range of interest. Data were analyzed using Fisons Instruments Opus software.

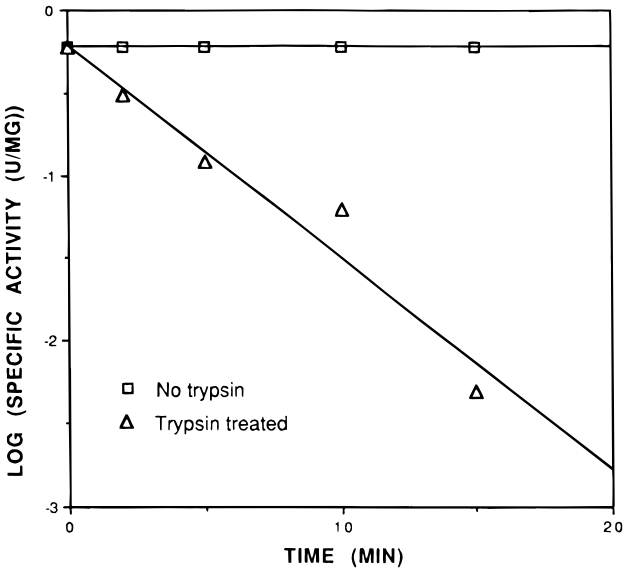

FIGURE 1: Kinetics of trypsin inactivation of NAPRTase. NAPRTase was incubated in the presence or absence of trypsin for the indicated periods of time as described in Experimental Procedures. The coupled ATPase activity of the enzyme was followed by the spectrophotometric assay as described (Vinitsky & Grubmeyer, 1993).

RESULTS

Overexpression and Purification of S. typhimurium NAPRTase. The *pncB* overexpressing construct pC18 (Vinitsky et al., 1991) contained upstream regulatory sequences [NadR (Holley et al., 1985) or NadI (Zhu et al., 1988) binding sequences] and gave unstable expression of *pncB*. PCR amplification of the *pncB* coding sequence from pC18 allowed its subcloning under T7 promoter control (pRM17.1) as described in Experimental Procedures. In order to maintain the stability of the *pncB* clone, pRM17.1 was always propagated in *S. typhimurium* RM926, and for growing large-scale cultures *S. typhimurium* RM926/pGP1-2 was transformed with pRM17.1. This procedure gave a high level overexpression of NAPRTase which allowed ready purification of the protein to apparent homogeneity in high yield (Experimental Procedures).

Proteolytic Cleavage of NAPRTase. NAPRTase catalyzes several distinct reactions (Vinitsky & Grubmeyer, 1993). The synthesis of NAMN can be measured as [^{14}C]NA incorporation under either ATP-coupled (ATP present) or uncoupled (ATP absent) conditions. ATP hydrolysis is measured under coupled (NA and PRPP present) or PP_i-stimulated (NA and PRPP absent and 1 mM PP_i present) conditions. The coupled ATPase activity of NAPRTase was extremely sensitive to trypsin. At a trypsin:NAPRTase ratio of 1:200, the loss of ATPase activity followed first-order kinetics (Figure 1), yielding a $t_{1/2}$ of 5 min and a $k_{inact} = 0.14$ min^{-1}. In an independent experiment, PP_i-stimulated ATPase activity was found to be lost in parallel with the coupled ATPase during trypsin treatment.

To determine whether the inactivation of ATPase activity resulted from relatively nonspecific damage to the NAPRTase protein, or from a more specific cleavage that damaged an ATPase domain, or from the coupling process itself, trypsin-treated NAPRTase was analyzed on 15% SDS−PAGE (Figure 2). Neither discrete secondary bands nor diminution of the primary protein band was observed. This result

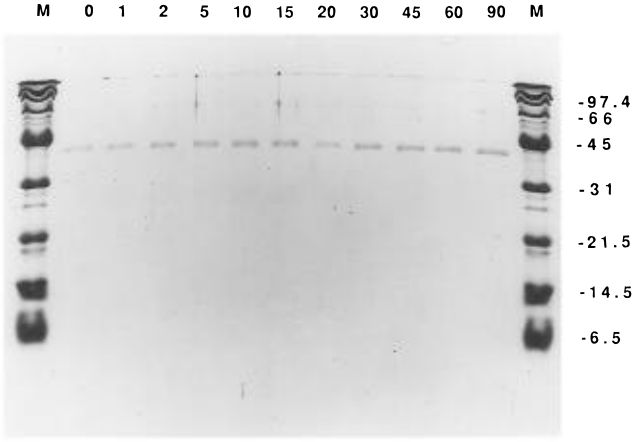

FIGURE 2: SDS−PAGE analysis of NAPRTase proteolysis. Tryptic digestion was carried out as described under Experimental Procedures, and 5 μg of digested protein from each inactivation time (min) was analyzed on 15% SDS−PAGE.

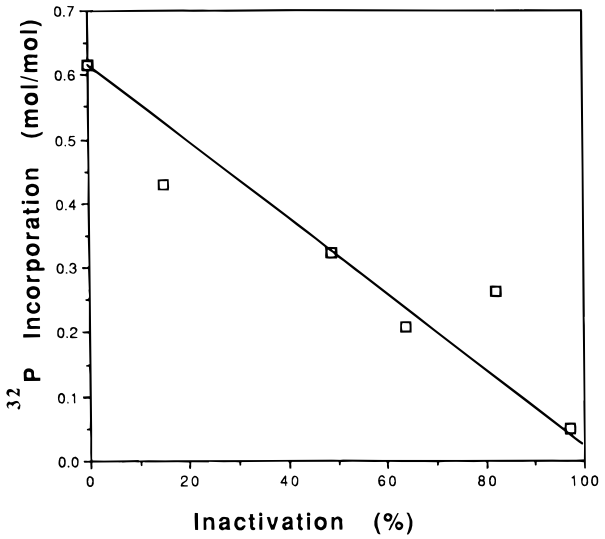

FIGURE 3: Phosphorylation of the trypsin-cleaved NAPRTase. Trypsin-treated NAPRTase inactivated to various levels of ATPase activity was incubated with [γ-^{32}P]ATP, and phosphorylation was analyzed as described under Experimental Procedures.

suggested that cleavage by trypsin was specific and occurred very near the amino or carboxy-terminal end of the protein. The specificity of the cleavage, its effect on activity, and ligand protection experiments described later led us to conduct a detailed investigation of the trypsin-cleaved enzyme.

It has been shown that ATP hydrolysis drives stoichiometric NAMN synthesis via phosphorylation of the enzyme at His-219 (Gross et al., accompanying paper). Phosphorylation of the enzyme after varying extents of trypsin inactivation was carried out using [γ-^{32}P]ATP in the presence of the stabilizing substrate PRPP. The loss of ATPase activity upon tryptic proteolysis was paralleled by loss of ability to phosphorylate the enzyme (Figure 3). Native NAPRTase catalyzes an ADP/ATP exchange (Vinitsky & Grubmeyer, 1993), providing a more powerful indicator of ATP utilization. Unproteolyzed enzyme gave an ADP/ATP exchange rate of 4.8 units/mg. No ADP/ATP exchange was observed in NAPRTase, whose ATPase activity had been 99% inactivated by trypsin treatment.

Trypsin Treatment Affects NAMN Synthesis. In order to understand whether separate domains of NAPRTase are

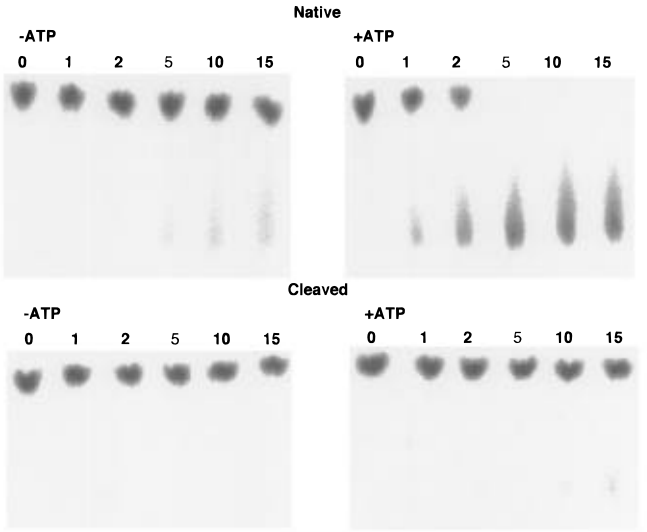

FIGURE 4: Conversion of [^{14}C]NA to [^{14}C]NAMN in trypsin-treated NAPRTase. Native and trypsin-treated NAPRTase (ATPase not detectable) were tested for NAMN synthesis using the radiolabel transfer assay (Experimental Procedures). The reaction was carried out in the presence and absence of ATP. Samples taken at different time intervals were separated on Whatman 3MM paper employing 1 M ammonium acetate, pH 5.0:ethanol (3:7). Numbers indicate reaction time in min.

responsible for ATPase and NAMN synthesis, NAMN synthesis by trypsin-treated NAPRTase was also followed with [^{14}C]NA. The quantification of the percentage conversion of the substrate, analyzed by thin-layer chromatography followed by phosphorimaging, yielded results comparable with those determined by scintillation counting. The experiments were carried out under coupled (+ATP) and uncoupled (−ATP) conditions for the native as well as for the cleaved enzyme (Figure 4). The rate of ATP-coupled NAMN synthesis, as well as the rate of coupled ATPase, was 100-fold lower for the cleaved enzyme than for the native enzyme, indicating the loss of both NAMN synthesis and ATP hydrolysis upon trypsin digestion. Uncoupled NAMN synthesis was no longer detectable with the cleaved enzyme. In a separate experiment, NAPRTase, whose coupled ATPase activity was inactivated to various extents by trypsin treatment, showed parallel loss of both coupled and uncoupled NAMN synthesis (data not shown).

Mapping of the Tryptic Cleavage. Trypsin-cleaved and native enzyme were each purified by HPLC, and identical amounts of each were then sequenced. Over the first six residues, identical quantities of the amino acids (Figure 5) representing the known amino-terminal Thr-Gln-Phe-Ala-Ser-Pro (Vinitsky et al., 1991) were found. The intact N-terminal sequence indicated that the site of specific tryptic cleavage was at the C-terminus.

To determine the size of the cleaved enzyme, we employed gel filtration on a calibrated column (1.6 × 60 cm) of Superdex-75. The elution volume (58 ± 0.35 mL) for the native protein (three independent determinations) was consistent with an M_r of ∼45 000. The cleaved enzyme (three independent determinations) eluted at 59 ± 0.3 mL, indicating an M_r of ∼40 000.

To define the trypsin cleavage site more precisely, the native and the cleaved enzymes were purified by reverse phase HPLC and analyzed by electrospray mass spectrometry (Table 2). Comparison of the observed mass values to

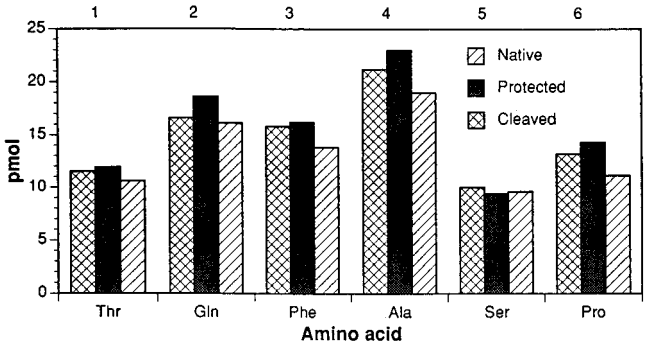

FIGURE 5: N-terminal sequencing of trypsin-cleaved NAPRTase. Samples were prepared as described under Experimental Procedures. Cycle numbers are indicated at the top of the figure.

Table 2: Electrospray Mass Spectrometry of Trypsin-Treated NAPRTase[a]

enzyme preparation	mass (Da) observed	predicted	cleavage site
native E			
Batch 1	45 542 ± 14	45 529	
Batch 2	45 533 ± 11	45 529	
cleaved E			
45%	43 846 ± 45	43 829	Arg-384
90%	42 686 ± 20	42 679	Lys-374
protected			
MgATP + MgPRPP	45 270 ± 14	45 243	Arg-396

[a] Samples were prepared as described in Experimental Procedures. The mass values observed were compared to the theoretical values calculated from the known amino acid sequence (Vinitsky et al., 1991) and assuming that cleavage occurred only after lysine or arginine.

theoretical values calculated from the known amino acid sequence (Vinitsky et al., 1991) using carboxy-terminal arginine or lysine residues as possible cut sites. The observed molecular mass for the native enzyme was 45 542 ± 14 Da which was nearly identical to the molecular mass of 45 529 [the molecular mass reported by Vinitsky et al. (1991) as 45 546 was incorrect] predicted from the amino acid sequence.

The observed molecular mass of the 90% inactivated trypsin cleaved peptide was 42 686 Da. The difference of 2856 Da (2850 Da predicted from the amino acid sequence) between the native and the cleaved enzyme identified the tryptic cut site as Lys-374 (underlined), which is 25 residues from the carboxy terminus.

^{374}KTICHDKAFVRALRKAFDLPQVRKAS-COOH^{399}

When partially cleaved (45% inactivated) protein was analyzed by electrospray mass spectrometry, three peptides were observed with molecular masses of 45 542 (native), 43 846, and 42 686 Da. The intermediate mass suggested that there could also be a cleavage site C-terminal to Lys-374. To investigate this possibility, a more detailed analysis of the C-terminal trypsin-generated fragments from the 45% inactivated sample was undertaken using matrix-assisted laser desorption time of flight (MALDI-TOF) mass spectrometry and employing the α-cyano-4-hydroxycinnamic acid matrix method (Experimental Procedures). Six smaller peptides were detected by this method with observed masses of 1700, 1542, 1413, 1189, 1074, and 945 Da. All of these masses are nearly identical to the predicted masses for tryptic peptide fragments arising from the C-terminus: Three are peptides

Table 3: Tryptic Digestion of NAPRTase in the Presence of Various Ligands

ligand[a]	$t_{1/2}$ (min)	k_{inact} (min^{-1})[b]
none	5	0.14
ATP	39	0.017
PRPP	19.5	0.035
ATP + PRPP	157.5	0.0044

[a] The ligands (1 mM) were added with equimolar concentrations of $MgSO_4$. [b] The rate constants for cleavage were calculated from the semilogarithmic plots derived from the time courses of tryptic digestion experiments.

starting at Ala-385 and extending to Ser-399 (1700.0), Lys-397 (1541.9), and Arg-396 (1413.7). Of the remaining three peptides, two had masses nearly identical to the predicted peptides starting at Ala-389 and extending to Lys-397 (1073.3) and Arg-396 (945.1). The observed mass of the remaining peptide was identical with the predicted mass of the peptide starting at Thr-375 and extending to Arg-384 (1189.4 amu). These results are consistent with an initial cleavage at Arg-384, resulting in an intermediate truncated protein (residues 1−384), which is observed as a molecular mass of 43 846 Da. Secondary cleavage at Lys-374 then produces the final 1−374 product.

Protection of NAPRTase against Proteolysis. The tryptic digestion of NAPRTase in the presence of various substrates (ATP, PRPP, and ATP with PRPP) was analyzed (Table 3) and rates compared with that for native enzyme. MgATP offered 8-fold protection against inactivation by trypsin. A 4-fold protection was observed with 1 mM MgPRPP. The presence of MgPRPP and MgATP together in the assay protected the enzyme to a greater extent (30-fold) than either ligand alone. Enzyme treated with trypsin in the presence of 1 mM MgPRPP and 1 mM MgATP for 30 min (94% remaining activity) was also analyzed by electrospray mass spectrometry. The observed molecular mass for the trypsin-treated protected sample was 45 270 Da and the difference of 276 ± 10 Da between the native and the protected sample suggested that the protected protein had been cleaved at Arg-396, removing the carboxy-terminal sequence ^{397}Lys-Ala-Ser^{399} (286 amu).

In order to understand whether the enzyme was protected against cleavage through phosphorylation or by ATP binding, ATP protection was examined in the absence of Mg^{2+} and with 2 mM EDTA added. Native enzyme failed to phosphorylate under these conditions; however, ATP protection against trypsin inactivation was still observed. These results indicated that phosphorylation of the enzyme was not needed for ATP to protect the enzyme against cleavage.

Cleavage by Chymotrypsin. Chymotrypsin was used to test the generality of our proposal that the carboxy-terminal of NAPRTase is exposed to solvent. Chymotrypsin digestion of NAPRTase at a weight ratio of 1:200, as for trypsin, also showed a first-order loss of ATPase activity. The presence of the substrates MgATP and MgPRPP at 1 mM levels (Table 4) offered 2.5- and 3-fold protection, respectively, but present together offered a 21-fold protection against inactivation. Chymotrypsin-inactivated NAPRTase also failed to phosphorylate when incubated with [γ-^{32}P]ATP. Chymotrypsin treatment also inactivated both the coupled and uncoupled NAMN synthesis reactions (Table 5) parallel to the loss of ATPase. SDS−PAGE of the chymotrypsin-cleaved samples did not reveal any shift in electrophoretic mobility compared to the native protein. Chymotrypsin-cleaved NAPRTase (63% inactivation for ATPase), and ATP and PRPP-protected enzyme (98% active) were freed from buffer and small peptides by reverse phase HPLC on a C4 column and analyzed by electrospray mass spectrometry to identify the chymotrypsin cleavage site. The apparent molecular mass of the chymotrypsin-inactivated cleaved peptide was 43 587 Da (Table 6), a difference of 1942 amu compared to the native protein (45 529 Da), indicating that cleavage had occurred at Phe-382, near the tryptic cleavage site at Lys-374. The molecular mass of the protected sample (45 534 Da) revealed that the enzyme had not been cleaved by chymotrypsin in the presence of ATP and PRPP.

In order to determine whether the ATP-induced conformational change observed on NAPRTase is global or local, other physical techniques were also employed. In gel filtration on Superdex-75 (1 × 30 cm), the unliganded and the liganded (+MgATP) enzyme eluted at the same volume (10.8 ± 0.05 mL). Fluorescence spectrometry of tryptophan (excitation = 295 nm) also did not reveal any change in the emission spectrum (emission max = 337 nm) between unliganded and liganded enzyme. To test thermal stability, the enzyme was incubated at 50 °C in 200 mM NaP_i, pH 8.0, 5% glycerol, and 2 mM DTT, and aliquots of the enzyme solution were assayed for the activity. There was a first-order loss of activity at this temperature for the unliganded enzyme ($t_{1/2}$ = 10 min) as well as for the liganded enzyme: MgATP ($t_{1/2}$ = 17 min), MgPRPP ($t_{1/2}$ = 8 min), and MgATP+MgPRPP ($t_{1/2}$ = 77 min), MgATP+EDTA ($t_{1/2}$ = 13.5 min).

Table 4: Chymotrypsin Digestion of NAPRTase in the Presence of Ligands

substrate[a]	$t_{1/2}$ (min)	k_{inact} (min^{-1})[b]
none	6.8	0.1
ATP	17.8	0.039
PRPP	17.8	0.034
ATP + PRPP	142	0.0048

[a] The ligands (1 mM) were added with equimolar concentrations of $MgSO_4$. [b] The rate constants of cleavage were calculated as described in Table 3.

Table 5: Conversion of [^{14}C]NA to [^{14}C]NAMN by Chymotrypsin-Treated NAPRTase

	coupled ATPase[a] (units/mg)	coupled NAMN synthesis[b] (units/mg)
native E	2.0	2.45
cleaved E	0.04	0.008

[a] Spectrophotometric assay and [b] radiotransfer assay (Experimental Procedures).

Table 6: Electrospray Mass Spectroscopy of Chymotrypsin-Treated NAPRTase[a]

	mass (Da)		
	observed	predicted	cleavage site
cleaved E	43 587 ± 10	43 594	Phe-382
protected E MgATP + MgPRPP	45 534 ± 14	45 529	

[a] The samples were prepared as described in Experimental Procedures. [b] The mass values observed were compared to the theoretical values calculated from the known amino acid sequence (Vinitsky et al., 1991) and assuming either that cleavage occurred after phenylalanine, tyrosine, and tryptophan residues or that it did not occur.

Chart 1

```
                                                  |         | |
Salmonella 367 PLNIVIKLVEC NGKPVAKLSD SPGKTICHDK AFVRALRKAF DLPQVRKAS 399
Yeast          PLNIVIKLLEV NGNHAIKISD NLGKNMG.DP ATVKRVKEEL GYTERSWSGD NEAHRWT
```

DISCUSSION

We have used limited proteolysis to detect ATP- and PRPP-dependent conformational changes in NAPRTase and suggest that these protein conformers may represent intermediate(s) in the unusual mode of energy coupling by this enzyme. It is known that when ATP is present, NAPRTase couples net ATP hydrolysis to conversion of NA and PRPP to NAMN and PP_i (Vinitsky & Grubmeyer, 1993). A step in this process is the phosphorylation of His-219 of the 399 residue protein (Gross et al., 1996). The presence of ATP lowers the K_M values for NA and PRPP, accelerates NAMN formation, and provides a steady-state displacement of the equilibrium between the substrates NA and PRPP and the products PP_i and NAMN. We have proposed that an enzyme conformer generated by an ATP-linked step is the enzyme form that binds substrates tightly and represents the specific catalyst of phosphoribosyl transfer, and that the high-affinity conformer reverts to the low-affinity form upon E-P cleavage, which is itself triggered by PP_i formation (Vinitsky & Grubmeyer, 1993). However, physical evidence for a separate conformer was lacking. The protection against proteolysis with ATP or PRPP and also the excellent protection offered when both ligands are present provide the first direct evidence that the enzyme undergoes a conformational change in response to ATP binding. On the basis of the rapid rate of the ATP/ADP exchange reaction, we have proposed that phosphorylation of NAPRTase and subsequent dissociation of ADP product precedes the development of the high-affinity state (Vinitsky & Grubmeyer, 1993). Steady-state kinetic studies (Kosaka et al., 1977; Hanna et al., 1983) indicated binding of PRPP and NA follows ATP binding, although these workers disagreed on whether enzyme phosphorylation and ADP dissociation precede PRPP and NA binding. The current results indicate that protection by ATP occurs even when phosphorylation is prevented by EDTA. The effective protection offered by ATP under conditions where no enzyme phosphorylation occurred demonstrates that the binding of ATP alone is sufficient to promote a conformational change that protects the enzyme against proteolysis. It is not yet clear whether the substrate-induced conformational change sensed by protease accessibility is the same as that which results in enzyme activation.

Mass spectrometry and amino acid sequencing established that the major stable product of tryptic digestion contained residues 1−374 of the 399-residue protein. In examination of the smaller proteolytic fragments, it became clear that Arg-384 was the initial cleavage site for trypsin, closely adjacent to the chymotrypsin cleavage site at Phe-382. Secondary trypsin cleavage at Lys-374, as well as degradation of the 385−399 fragment, occurred rapidly. The susceptibility of the Phe-382 to Arg-384 region to two distinct proteases demonstrates that the region is solvent-exposed in the unliganded protein. None of the Arg-384, Phe-382, or Lys-374 sites was available in the ATP/PRPP-protected enzyme, demonstrating that a conformational change occurs on substrate binding. In known three-dimensional structures of OPRTase and HGPRTase the active sites are highly solvent-exposed, and it has been proposed that nearby flexible peptide loops move to cover the active site during catalysis (Scapin et al., 1994; Eads et al., 1994). In creatine kinase (Wyss et al., 1993) and γ-aminobutyrate transporter (Mabjeesh & Kanner, 1993) similar protease sensitivity experiments were also interpreted to indicate solvent exposure and substrate-induced conformational changes.

A number of properties of the cleaved NAPRTase indicate that it has not been globally damaged by proteolysis and that it maintains a compact structure. The first of these is the observation that proteolysis stops after cleavage at Lys-374. Longer proteolysis or addition of trypsin in ratios of 1:10 failed to yield further degradation, demonstrating that the enzyme had not become denatured by the initial cleavage. Secondly, gel filtration chromatography of the cleaved enzyme revealed a smaller size, consistent with a compact folded structure remaining after the proteolytic event. Finally, in unpublished studies, our collaborators have been able to produce microcrystals of the cleaved form of the enzyme (J. Eads and J. C. Sacchettini, personal communication), suggesting that it maintains a defined structure.

The trypsin-sensitive carboxy-terminal region of NAPRTase may play a direct role in energy-coupled catalysis. In yeast phosphoglyceromutase, the 10-residue carboxy terminal is stabilized by substrate binding, and its removal by limited proteolysis inactivates the enzyme (Winn et al., 1981). In that case, as with NAPRTase, a phosphohistidine intermediate (His-8 in phosphoglyceromutase) occurs, and on the basis of the known three-dimensional structure, the carboxy-terminal residues are predicted to interact with the phosphohistidine (Winn et al., 1981). One would expect that if the carboxy terminal region of NAPRTase were catalytically significant, it might show good sequence identity between species. The only other published sequence is for the *Escherichia coli* NAPRTase (Wubbolts et al., 1990), which shared high sequence similarity. An unpublished sequence of the yeast NAPRTase (kindly provided by Drs. Dominique Lalo and Pierre Thuriaux, CEA, Saclay, France), when aligned with the *Salmonella* sequence, reveals that sequence identity (underlining; cleavage sites are denoted with vertical bars) and conservative replacement is stronger preceding the secondary tryptic cleavage site at Lys-374 (see Chart 1). It may be that positioning of the peptide region preceding Lys-374 is critical for enzymatic catalysis.

We have previously suggested that residues 373−375 of NAPRTase might represent part of an ATP-binding motif (Vinitsky et al., 1991), although similarity to archetypal ATP-binding sequences is weak. In the current work, it was clear that proteolysis of NAPRTase inactivated all processes involving ATP, including ATPase activity, the net phosphorylation of the enzyme, and the ATP/ADP exchange reaction. The latter two of these processes do not require either of the substrates for the PRTase reaction. Arguing against the

exclusive assignment of the carboxy terminal to ATP binding is the finding that the uncoupled synthesis of NAMN was also inactivated by proteolytic cleavage in parallel to the loss of ATPase activity. Since the uncoupled NAMN synthesis occurs in the absence of ATP, one might presume that it does not require participation of the ATP site.

NAPRTase is unusual among metabolic enzymes in using indirect coupling between ATP hydrolysis and NAMN synthesis. To our knowledge this behavior is paralleled only by that of ATP sulfurylase (Liu et al., 1994). The chemical and protein structural details of energy coupling in NAPRTase may provide insight into the ATP-driven recognition processes of a number of other enzymes.

REFERENCES

Ames, G. F.-L. (1990) in *The Bacteria XII: Bacterial Energetics* (Krulwich, T. A., Ed.) pp 225−246, Academic Press, New York.

Armon, T., Ganoth, D., & Hershko, A. (1990) *J. Biol. Chem. 265*, 20723−20726.

Cullis, P. M., Maxwell, A., & Weiner, D. P. (1992) *Biochemistry 31*, 9642−9646.

Davis, R. W., Bostein, D., & Roth, J. R. (1980) *Advanced Bacterial Genetics*, Cold Spring Laboratory, Cold Spring Harbor, NY.

Eads, J. C., Scapin, G., Xu, Y., Grubmeyer, C., & Sacchettini, J. C. (1994) *Cell 78*, 325−334.

Gross, J., Rajavel, M., Segura, E., & Grubmeyer, C. (1996) *Biochemistry 35*, 3917−3924.

Hanna, L. S., Hess, S. L., & Sloan, D. L. (1983) *J. Biol. Chem. 258*, 9745−9754.

Holley, E. A., Spector, M. P., & Foster, J. W. (1985) *J. Gen. Microbiol. 131*, 2759−2770.

Jencks, W. P. (1980) *Adv. Enzymol. 51*, 75−106.

Jencks, W. P. (1989) *J. Biol. Chem. 264*, 18855−18858.

Khan, V., & Blum, J. J. (1967) *Biochem Biophys. Acta. 146*, 305−308.

Kosaka, A., Spivey, H. O., & Gholson, R. K. (1971) *J. Biol. Chem. 246*, 3277−3283.

Kosaka, A., Spivey, H. O., & Gholson, R. K. (1977) *Arch. Biochem. Biophys. 179*, 334−341.

Liu, C., Martin, E., & Leyh, T. S. (1994) *Biochemistry 33*, 2042−2047.

Mabjeesh, N. J., & Kanner, B. I. (1993) *Biochemistry 32*, 8540−8546.

Martin, J., Langer, T., Botera, R., Schramel, A., Horwich, A. L., & Hartl, F. U. (1991) *Nature 352*, 36−42.

Meek, T. D., & Villafranca, J. J. (1982) *Biochemistry 21*, 2158−2167.

Nguyen, T. T., Muench, K. A., & Bryant, F. R. (1993) *J. Biol. Chem. 268*, 3107−3113.

Niedel, J., & Dietrich, L. S. (1973) *J. Biol. Chem. 248*, 3500−3505.

Penefsky, H. S. (1977) *J. Biol. Chem. 252*, 2891−2899.

Preiss, J., & Handler, P. (1958) *J. Biol. Chem. 233*, 492−500.

Sambrook, J., Fritsch, E. F., & Maniatis, E. F. (1989) *Molecular Cloning, A Laboratory Manual*, Cold Spring Laboratory, Cold Spring Harbor, NY.

Scapin, G., Grubmeyer, C., & Sacchettini, J. C. (1994) *Biochemistry 33*, 1287−1294.

Smith, J. L., Zaluzec, E. J., Wery, J., Niu, L., Switzer, R. L., Zalkin, H., & Satow, Y. (1994) *Science 264*, 1427−1433.

Smith, L. D., & Gholson, R. K. (1969) *J. Biol. Chem. 244*, 68−71.

Stitt, B. L. (1988) *J. Biol. Chem. 263*, 11130−11137.

Szabo, A., Langer, T., Schroder, H., Flanagan, J., Bukau, B., & Hartl, U. (1994) *Proc. Natl. Acad. Sci. U.S.A. 91*, 10345−10349.

Tabor, S., & Richardson, C. (1985) *Proc. Natl. Acad. Sci. U.S.A. 82*, 1074−1078.

Tanford, C. (1983) *Annu. Rev. Biochem. 52*, 379−409.

Vinitsky, A., & Grubmeyer, C. (1993) *J. Biol. Chem. 268*, 26004−26010.

Vinitsky, A., Teng, H., & Grubmeyer, C. T. (1991) *J. Bacteriol. 173*, 536−540.

West, S. C. (1992) *Annu. Rev. Biochem. 61*, 603−640.

Winn, S. I., Watson, H. C., Harkins, R. N., & Fothergill, L. A. (1981) *Phil. Trans. R. Soc. London B 293*, 121−130.

Wyss, M., James, P., Schlegel, J., & Wallimann, T. (1993) *Biochemisty 32*, 10727−10735.

Wubbolts, M. G., Terpstra, P., van Beilen, J., Kingma, J., Meesters, H. A. R., & Withholt, B. (1990) *J. Biol. Chem. 265*, 17665−17672.

Yodh, J. G., & Bryant, F. R. (1993) *Biochemistry 32*, 7765−7771.

Zhu, N., Olivera, B. M., & Roth, J. R. (1988) *J. Bacteriol. 170*, 117−125.

BI951791Y